Eardrum and columella displacement in single ossicle ears under quasi-static pressure variations

Reference:
Claes Raf, Muyshondt Pieter, Van Assche Frederic, Van Hoorebeke Luc, Aerts Peter, Dirckx Joris.- Eardrum and columella displacement in single ossicle ears under quasi-static pressure variations
Hearing research - ISSN 0378-5955 - 365(2018), p. 141-148
Full text (Publisher's DOI): https://doi.org/10.1016/J.HEARES.2018.05.012
To cite this reference: https://hdl.handle.net/10067/1531490151162165141

Eardrum and columella displacement in single ossicle ears under quasi-static pressure variations

Raf Claes[1,2], Pieter G.G. Muyshondt[3], Frederic Van Assche[4], Luc Van Hoorebeke[4], Peter Aerts[1,5], Joris J.J. Dirckx[3]

[1] University of Antwerp, Laboratory of Functional Morphology, Universiteitsplein 1, B-2610 Antwerp, Belgium
[2] Vrije Universiteit Brussel, Department of Mechanical Engineering, Pleinlaan 2, B-1050 Brussels, Belgium
[3] University of Antwerp, Laboratory of BioMedical Physics, Groenenborgerlaan 171, B-2020 Antwerp, Belgium
[4] Ghent University, UGCT – Radiation Physics, Department of Physics and Astronomy, Proeftuinstraat 86, B-9000 Ghent, Belgium
[5] Ghent University, Department of Movement and Sport Science, Watersportlaan 2, B-9000 Ghent, Belgium

Email: **raf.claes@uantwerpen.be** (corresponding author)

Abstract

Although most birds encounter large pressure variations during flight, motion of the middle ear components as a result of changing ambient pressure are not well known or described. In the present study, motion of the columella footplate and tympanic membrane (extrastapedius) in domestic chickens (*Gallus gallus domesticus*) under quasi-static pressure conditions are provided. Micro-CT scans were made of cadaveric heads of chickens under positive (0.25 kPa, 0.5 kPa, 1 kPa, and 1.5 kPa) and negative (-0.25 kPa, -0.5 kPa, -1 kPa, and -1.5 kPa) middle ear pressure. Both extrastapedius and columella footplate displacements show a non-linear S-shaped curve as a function of pressure indicating non-linear response characteristics of the middle ear components. The S-curve is also seen in mammals, but unlike in mammals, the lateral piston-like displacement of both the columella footplate and extrastapedius, which is caused by an increased middle ear pressure are smaller than the medial piston-like displacements, caused by a decreased middle ear pressure of the same magnitude. Columella footplate piston displacements are always smaller than the extrastapedius piston displacements, indicating the flexibility of the extracolumella. The cone-shape of the avian tympanic membrane with inverted apex in comparison to the mammalian tympanic membrane can cause the inverted shape of the pressure response curve.

Keywords: avian middle ear, middle ear pressure, columella, tympanic membrane, micro-CT scanning, chicken

Abbreviations

ME: middle ear

1 Introduction

In mammals the middle ear (ME) cavity is enclosed within one single bony structure and is sealed off by the tympanic membrane. The only connection to the pharynx is via the Eustachian tubes. The mammalian ME contains three bony ossicles (malleus, incus, and stapes), two muscles (tensor tympani muscle and stapedius muscle), and some ligaments (anterior and superior mallear ligament, posterior incudal ligament, and the annular ligament) (Møller, 1974, Rosowski, 1996, Ades et al., 2012). The mammalian tympanic membrane is conically shaped with the tip, where it connects with the umbo of the malleus, pointing medially (Decreamer et al., 1991). Both slow and sudden pressure changes cause a pressure differential over the tympanic membrane which deforms and displaces, altering the mechanical behavior and configuration of the chain of ossicles. These effects may alter the acoustic transfer function (Murakami et al., 1997; Teoh et al., 1997; Rosowski and Lee, 2001; Dirckx et al., 2006). The effects of changing static pressure on the mammalian ME have been investigated in detail (Hüttenbrink, 1988; Dirckx and Decreamer, 1991; Dirckx et al., 2006). Experiments conducted by Dirckx et al. (2006) on cadaveric rabbit temporal bones, for example, show an umbo displacement of 165 µm when pressure was raised and decreased 2.5 kPa above and below ambient pressure, while the stapes displacement was only 34 µm.

The behavior of the avian ME under static pressure conditions is known in much less detail. The avian ME cavity is enclosed within two bony structures (the cranium and quadratum) and is sealed off by the tympanic membrane. MEs on both side of the head are connected to each other by intracranial air-filled cavities and the interaural pathway (fig. 1a). MEs are connected to the outside world (nasopharynx) via the Y-shaped pharyngotympanic tube which is a part of the interaural pathway (Wada, 1923; Schwartzkopff, 1955; Counter and Borg, 1979). Under normal conditions, this tube is closed (Claes et al., 2017). The ME contains one ossicle with a bony shaft (the columella) and a cartilaginous, trifurcated distal end (the extracolumella consisting of the extrastapedius, infrastapedius, and suprastapedius), some ligaments (ascendens ligament, drumtubal ligaments, Platner's ligament, and annular ligament), and one muscle (tympanic muscle) (fig. 1b) (Smith, 1904; Starck, 1995; Saunders et al., 2000). The avian tympanic membrane is conically shaped with the tip pointing laterally (Saunders et al. 2000). In birds, only one study provides quantitative data on deformations and motion of the columella footplate over a range of ME pressures (Arechvo et al., 2013). In other studies only descriptive data or data with only one pressure condition in the ME are provided (Pohlman, 1921; Gaudin, 1968; Norberg, 1978; Claes et al., 2017; Muyshondt et al., 2018). Although most birds encounter large pressure variations during flight, little data exist on the motion of the tympanic membrane and columella under static pressure loads.

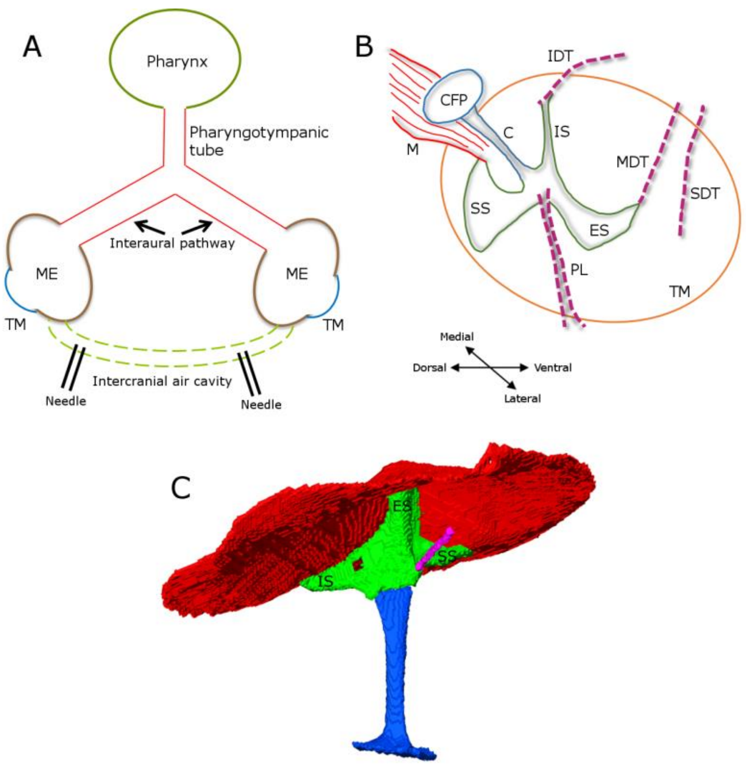

Figure 1: A) schematic overview of the connections between the pharynx and middle ears in birds (ME), showing the pharyngotympanic tube, interaural pathway, intercranial air cavities (with indication of the needles), and tympanic membrane (TM). B) Schematic medial view of the ME components: tympanic membrane (TM), columella (C), columella footplate (CFP), extrastapedius (ES), infrastapedius (IS), suprastapedius (SS), Platner's ligament (PL), superior drumtubal ligament (SDT), medial drumtubal ligament (MDT), inferior drumtubal ligament (IDT), and tympanic muscle (M). Deduced from Smith (1904). C) chicken's ME components: tympanic membrane: red; extracolumella: green; columella: blue; Platner's ligament: purple.

Two theories stand on how the columella displaces under quasi-static and dynamic pressure loads exerted on the deforming tympanic membrane. The first theory describes the motion of the columella footplate as an inward and outward piston-like motion (Pohlman, 1921; Norberg, 1978; Manley, 1990). Pohlman (1921) attributes this motion to a rotation of the extracolumella and columella at the intercolumellar joint. Norberg (1978) describes the motion as originating from a rotation about the axis of rotation of the extracolumella located at the rim of the tympanic membrane. Manley (1990) describes that the motions does not take place by a rotation at the intercolumellar joint but within the flexible extracolumella itself. The second theory describes the motion of the columella footplate as being a rocking motion (Gaudin, 1968), caused by the acute angle between the shaft of the columella and the tympanic membrane, the out-of-center attachment of the columella shaft to the columella footplate, and the asymmetrical anatomy of the annular ligament of the columella being wider at the anterior edge of the columella footplate.

In the present study we measured pressure induced deformations and motion of the tympanic membrane and columella by means of micro-CT scanning to quantify the nature of these motions.

2 Materials and methods

2.1 Sample preparation

Four heads (from now on referred to as C1, C2, C3, and C4) of adult domestic chickens (*Gallus gallus domesticus*) were obtained from a chicken farm and prepared the same day for scanning. Two hypodermic needles (diameter: 0.8 mm), attached to a rubber tube, were inserted in the caudal part of the skull (fig. 1a). Through one needle air was injected to or extracted from the intracranial air cavities, interaural pathway, and hence the MEs to change the pressure. Through the second needle, pressure within the MEs was measured with a pressure gauge. Glue was applied around the entrance point of the needles into the skull to ensure the system was airtight. The heads were stored in a refrigerator at a temperature of 5°C for one night with a water-soaked paper to ensure the samples did not dry out.

2.2 Micro-CT scanning

Micro-CT scans were made with the Environmental Micro-CT (EMCT) by the Centre for X-ray Tomography at Ghent University (Dierick et al., 2014). In this system, contrary to standard micro-CT scanners, the source and detector rotate around the stationary object in the horizontal plane. As such, the connection between peripheral equipment and the object is much more straightforward and stable. Nine scans were made per head, each with a different middle ear pressure. During the first scan the needle was left open to the atmosphere to ensure that ambient and ME pressure were identical. Next, the fine needle was connected with a rubber tube to a custom-made pressure generator which continuously maintained the pressure at the required level. ME pressure was set at 0.25 kPa, 0.5 kPa, 1 kPa, and 1.5 kPa above ambient pressure and then at -0.25 kPa, -0.5 kPa, -1 kPa, and -1.5 kPa. When ME pressure was altered scanning was postponed for 2 minutes so that deformations could stabilize before the start of the scan. All samples were scanned over an angle of 360° with the X-ray source set at 90 kV. For C1 and C2 the exposure time was set at 40 ms and total scanning time per sample was 7 minutes. Due to technical changes at the scanner facility, the second set of heads (C3 and C4) was scanned with slightly different settings: exposure time was set at 60 ms and total scanning time per sample was 10 minutes. The reconstructed slice images had a voxel size of 29.34 µm (C1 and C2) and 24.7 µm (C3 and C4).

2.3 Data analysis and measurements

A three-dimensional processing software package (AMIRA 5.4.4.; 64-bit version) was used to assign the voxels corresponding to the tympanic membrane, columella, extracolumella, and the bony semi-circular canals of the inner ear. Segmentation was performed by automatic thresholding based on grey-scale values in combination with a manual correction in the three orthogonal views. The segmented outlines were smoothed and a surface model was created. The bony semi-circular canals of the inner ear were used to align the models so a comparison could be made between the different pressure conditions.

Possible deformations of the tympanic membrane were visualized by taking the cross-section of the membrane (for +1.5 kPa and -1.5 kPa) in the longitudinal direction through the tip where the extrastapedius pushes the tympanic membrane outwards. For individual C4 the cross-section was shown for the different pressure conditions. Deformations were also measured at the apex of the extrastapedius. Potential translation of the columella was assessed by allocating four anatomical points on the rim of the footplate. The mean of the coordinates per pressure condition was calculated for all nine pressure conditions and subtracted from the 0 kPa condition. The linear displacement of the tips of the extracolumella (infra-, extra-, and suprastapedius) were also measured. Negative values indicate a medial displacement while positive displacements indicate a lateral movement. The piston-like component of the extracolumella and columella footplate displacements is plotted as a function of ME pressure. In what follows we will refer to this as the "linear motion", not to be confused with the non-linear response of the motion amplitude as function of pressure. Columella angular rotations were measured as the rotation of the lateral end of the bony shaft relative to the columella footplate center point.

3 Results

3.1 Tympanic membrane deformation

Fig. 2 shows the full field deformation of the tympanic membrane of C4 at a ME pressure of +1.5 kPa (fig. 2a) and -1.5 kPa (fig. 2b). Fig. 3 displays cross-sections of the tympanic membrane, at different ME pressures, in the longitudinal direction through the tip where the extrastapedius pushes the tympanic membrane outwards (fig. 3d). The maximal lateral displacement of the tip of the tympanic membrane, when ME pressure is increased, is limited by the position of the extrastapedius (fig. 3a). The largest lateral deformation is observed at the ventral side of the tympanic membrane, where the distance of the tip of the tympanic membrane and the edge is maximal. When ME pressure is decreased 1.5 kPa below ambient a medial deformation of the tympanic membrane is observed. The ventral side of the tympanic membrane undergoes the largest deformation (fig. 3b). Differences between the left and right tympanic membrane are rather small and may be caused by small differences in degree of ossification of the (extra)columella or by a small difference in stiffness of the tympanic membranes. A small increase of ME pressure (0.25 kPa) induces a major portion of the maximal deformation. At a ME pressure of -0.25 kPa, only a small eardrum displacement is observed. Decreasing ME pressure further causes the tympanic membrane to bulge inward (fig. 3c).

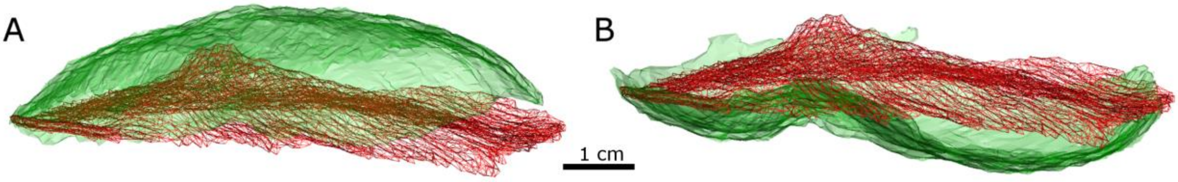

Figure 2: Edge view of the right tympanic membrane of C4. A) Comparison of ambient ME pressure and increase of ME pressure by 1.5 kPa. B) Comparison of ambient ME pressure and decrease of ME pressure by 1.5 kPa. Color code: green: increased and decreased ME pressure; red: ambient ME pressure.

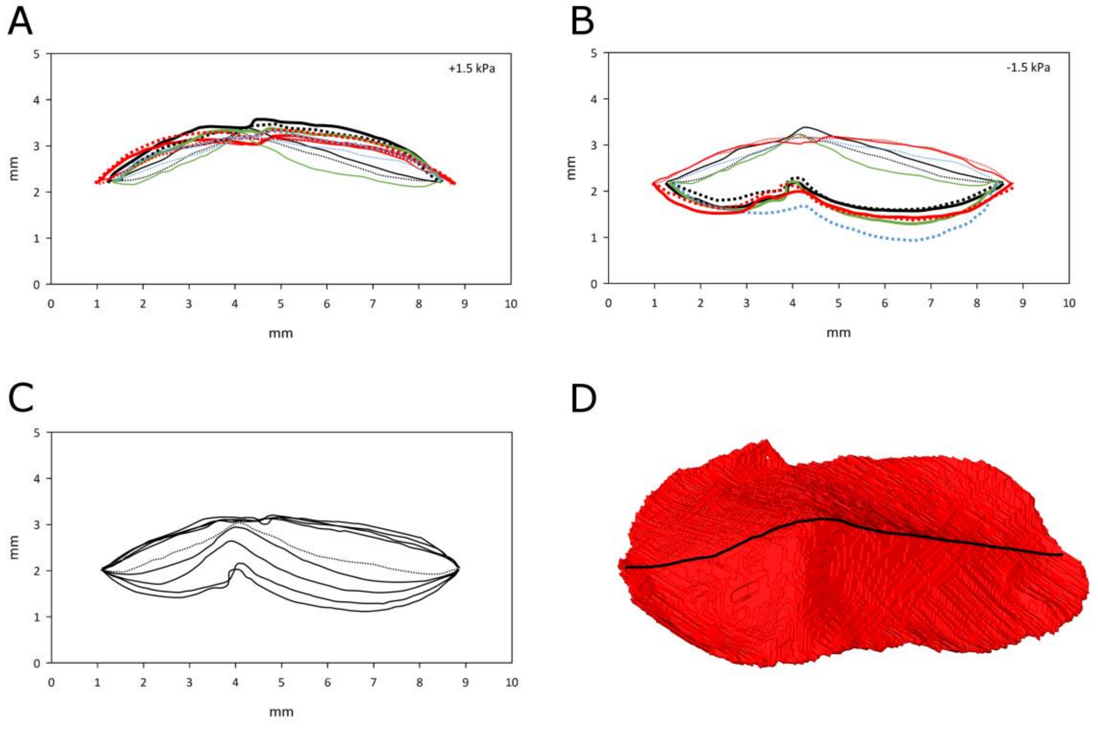

Figure 3: Cross-section of the tympanic membrane in the longitudinal direction through the tip where the extrastapedius pushes the tympanic membrane outwards with ME pressure increased 1.5 kPa above ambient pressure (A) and decreased 1.5 kPa below ambient pressure (B). Full line: left tympanic membrane; dashed line: right tympanic membrane. The different colors indicate the 4 different individuals (black: C1; red: C2; blue: C3; green: C4). Thin graphs: cross-section of the tympanic membrane with ambient ME pressure; thick graphs: changed ME pressure C) Cross-section of the tympanic membrane of C4 with the different ME pressures (full lines; dashed line: ambient ME pressure). D) Schematic indication of position of the cross-section on a tympanic membrane.

3.2 Columella and extracolumella displacement

Fig. 4 shows 3-D representations of the columella and extracolumella at rest position and for the different pressure conditions. Table 1 summarizes the quantitative results. When ME pressure was increased 0.25 kPa above ambient pressure a small lateral displacement of the columella footplate (0.04 ±0.04 mm), extra- (0.07 ±0.07 mm), and infrastapedius (0.03 ±0.08 mm) was observed. The displacement occurs in the direction parallel to the shaft of the columella, and from here on we will refer to it as piston displacement. No displacement of the suprastapedius was detected. When ME pressure was further increased to 0.5 kPa above ambient pressure, spatial configuration of both the columella and extracolumella remained unchanged. An increase in lateral piston displacement of both the infra- (0.07 ±0.11 mm) and suprastapedius (0.03 ±0.08 mm) was measured. When ME pressure was raised 1 kPa above ambient pressure the lateral displacement of the columella (0.05 ±0.04 mm), extra- (0.12 ±0.11 mm), infra- (0.09 ±0.13 mm), and suprastapedius (0.04 ±0.09) increased. When the pressure was further increased to 1.5 kPa above ambient pressure an increase in piston displacement of the columella footplate could be observed resulting in a total piston displacement of 0.07 ±0.05 mm. A large increase in the displacement of the infrastapedius was present resulting in a total displacement of 0.26 ±0.19 mm. Very small columella footplate rotations of 0.3 ±0.4°, 0.3 ±0.6°, 0.5 ±0.9°, and 1.1 ±1.0° could be observed for an increased ME pressure of respectively 0.25 kPa, 0.5 kPa, 1 kPa, and 1.5 kPa (fig. 4a and 5, table 1).

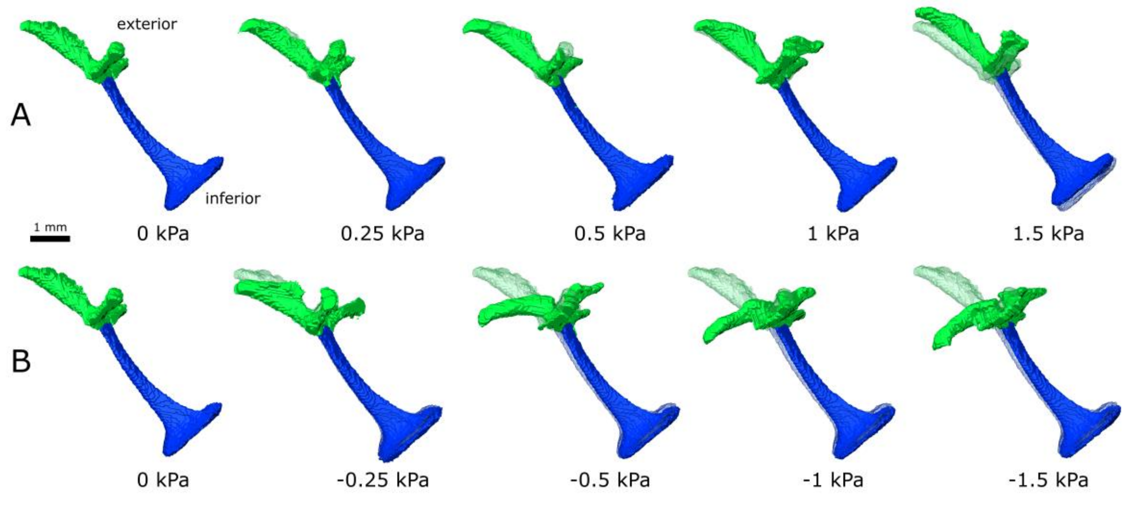

Figure 4: Dorsal view of deformations and translations of the columella (blue) and extracolumella (green) under an increased (A) and decreased (B) ME pressure. The transparent surface represents the condition at ambient ME pressure. Opaque surfaces represent the shape of the columella and extracolumella when deformed by ME pressure changes.

When ME pressure was decreased 0.25 kPa below ambient pressure, a medial piston movement of the columella footplate (0.09 ±0.01 mm), extra- (0.25 ±0.18 mm), infra- (0.25 ±0.14 mm), and suprastapedius (0.15 ±0.16 mm) could be observed. These translations had a similar magnitude as the lateral translation at 1.5 kPa. When ME pressure was further decreased to 0.5 kPa below ambient pressure, the medial translation increased to 0.11 ±0.07 mm, 0.94 ±0.37 mm, 0.27 ±0.20 mm, and 0.39 ±0.20 mm for the columella, extra-, supra-, and infrastapedius respectively. When ME pressure was decreased 1 kPa below ambient pressure, no further increase in medial piston translation of the columella footplate could be observed. An increase in medial piston translation of the three arms of the extracolumella was noticed (extrastapedius: 1.32 ±0.34 mm, suprastapedius: 0.29 ±0.22 mm, and infrastapedius: 0.42 ±0.17 mm). When ME pressure was further decreased to 1.5 kPa below ambient pressure no further piston movement of the columella footplate, infra-, and suprastapedius was observed. A further medial translation of the tip of the extrastapedius was measured resulting in a total piston displacement of -1.41 ±0.31 mm. Very small columella footplate rotations of 1.1 ±0.9°, 1.1 ±0.8°, 1.7 ±1.2°, and 2.1 ±1.1° could be observed for a decreased ME pressure of 0.25 kPa, 0.5 kPa, 1 kPa, and 1.5 kPa respectively (fig. 4b and 5, table 1). Figure 5 includes umbo and stapes displacements of mammalian species (New Zealand White rabbit (Dirckx et al., 2006), human (Hüttenbrink, 1988; Dirckx and Decreamer, 1991), and gerbils (Dirckx and Decreamer, 2001)) and one avian species (common ostrich (Arechvo et al., 2013)). The stapes footplate displacement in mammals is much smaller than the columella motion. Therefore fig. 5c and 5d show plots where the amplitude range of the mammal data were scaled to the same range as the columella data of the chicken so that the shape of the curves can be better compared. Both umbo and stapes displacement value were multiplied with a scaling factor (maximal amplitude chicken / maximal amplitude mammal) to scale the mammalian amplitude ranges. The scaling factors for the umbo displacement were 0.125, 0.5, and 0.3 for respectively New Zealand white rabbit, human, and gerbil. The scaling factors for the stapes displacement were 0.035 and 0.018 for respectively New Zealand white rabbit and human. The literature data on ostrich are only available for positive pressures, hence they were omitted in the scaled representation of fig. 5c and 5d.

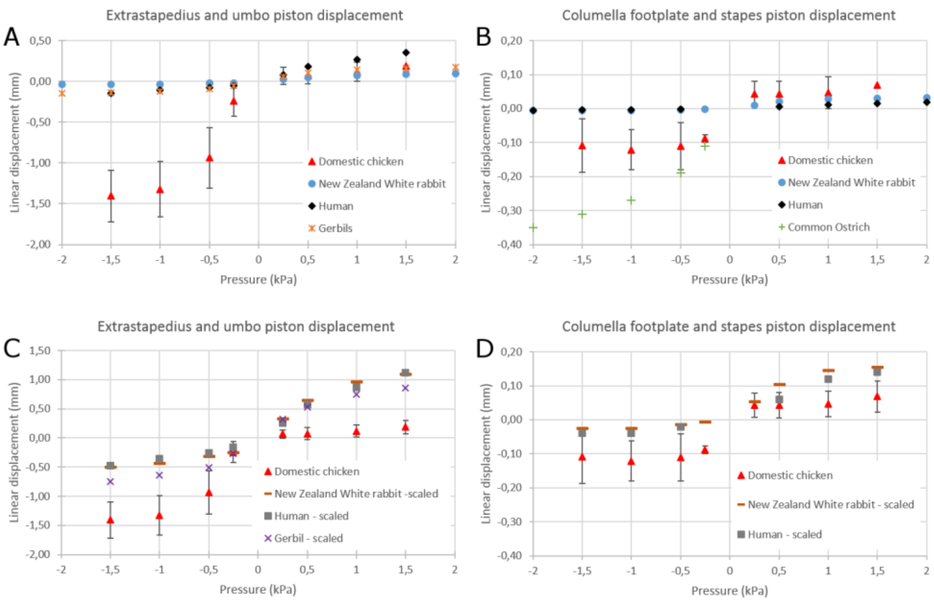

Figure 5: Extrastapedius and umbo (A) and columella footplate and stapes (B) piston displacements as a function of ME pressure. Extrastapedius and scaled umbo (C) and columella footplate and scaled stapes (D) piston displacement as function of ME pressure. Data for New Zealand White rabbit are taken from Dirckx et al., 2006, human from Hüttenbrink (1988); Dirckx and Decreamer (1991), gerbil from Dirckx and Decreamer (2001), and common ostrich from Arechvo et al. (2013). In (C) and (D) the mammal data are scaled so that the total amplitude range is equal to the amplitude range measured in chicken. The literature data on ostrich are only available for positive pressures, hence they are omitted in the scaled representation of (C) and (D).

Peak-to-peak displacement (sum of the piston displacement at 1.5 kPa and -1.5 kPa ME pressure) of the columella footplate, extra-, infra-, and suprastapedius with an increase and decrease of 1.5 kPa in ME pressure were respectively, 0.15, 1.48, 0.49, and 0.30 mm. The lateral displacement of the columella footplate caused by a raise of ME pressure was respectively 2.3, 2.8, 2.4, and 1.6 times smaller than the medial displacement caused by a decrease in ME pressure of the same magnitude (0.25 kPa, 0.5 kPa, 1 kPa, and 1.5 kPa). The lateral displacement of the extrastapedius was respectively 3.4, 13.4, 11, and 7.4 times smaller than the medial displacement caused by a decrease in ME pressure of the same magnitude (0.25 kPa, 0.5 kPa, 1 kPa, and 1.5 kPa).

Table 1: Mean and standard deviation (SD) of the piston displacement of the columella footplate (CFP), extrastapedius (ES), suprastapedius (SS) and infrastapedius (IS) in mm and rotation angles of the columella in ° for the different pressure conditions. Positive values indicate a lateral displacement. Negative values indicate a medial displacement.

	CFP (mm)		ES (mm)		SS (mm)		IS (mm)		Rotation (°)	
kPa	**Mean**	**±SD**	**Mean**	**±SD**	**Mean**	**±SD**	**Mean**	**±SD**	**Mean**	**±SD**
1.5	0.07	0.05	0.19	0.12	0.09	0.11	0.26	0.19	1.1	1.0
1	0.05	0.04	0.12	0.11	0.04	0.09	0.09	0.13	0.5	0.9
0.5	0.04	0.04	0.07	0.10	0.03	0.08	0.07	0.11	0.3	0.6
0.25	0.04	0.04	0.07	0.07	0.00	0.00	0.03	0.08	0.3	0.4
-0.25	-0.09	0.01	-0.24	0.18	-0.15	0.16	-0.25	0.14	1.1	0.9
-0.5	-0.11	0.07	-0.94	0.37	-0.27	0.20	-0.39	0.20	1.1	0.8
-1	-0.12	0.06	-1.32	0.34	-0.29	0.22	-0.42	0.17	1.7	1.2
-1.5	-0.11	0.08	-1.41	0.31	-0.30	0.22	-0.46	0.19	2.1	1.1

4. Discussion

The effects of ambient pressure fluctuations on the ME components are well known and described in different mammalian species. New Zealand white rabbits showed a stapes displacement of 30 µm and umbo displacement of 100 µm after lowering the pressure in the auditory canal with 1.5 kPa (Dirckx et al., 2006). When pressure was raised 1.5 kPa a stapes displacement of 7 µm and umbo displacement of 35 µm was measured. Umbo displacements are 3.57 times larger than the stapes displacement amplitude. In humans, a stapes displacement of 14 µm and umbo displacement of 350 µm was observed after the pressure in the auditory canal was decreased 1.5 kPa. When pressure was increased with the same magnitude the stapes displaced 4 µm and the umbo 150 µm (Hüttenbrink, 1988; Dirckx and Decreamer, 1991). The displacement of the umbo is 23 times larger than the stapes displacement amplitude (Dirckx and Decreamer, 2001). Decreasing pressure 1.5 kPa in the gerbil's auditory canal causes the umbo to displace 175 µm. When pressure is increased by the same magnitude the umbo displaced 125 µm (Dirckx and Decreamer, 2001). In mammals both umbo and stapes displacements caused by ambient pressure fluctuations show non-linear S-shaped curves which indicate the non-linear response characteristics of the ME components. Magnitudes of umbo and stapes displacement at overpressure in the auditory canal are always significantly larger than the displacement at negative pressure of the same magnitude. The asymmetric shape of the curves of the umbo and stapes displacement curves as function of pressure can possibly be attributed to the conical shape of the tympanic membrane. Due to its shape, the tympanic membrane stretches at overpressure in the auditory canal but can easily bend and balloon outward at negative pressure.

Although birds are frequently exposed to ambient pressure changes due to their lifestyle, only one study provides quantitative data on deformations and motion of the columella footplate over a range of ME pressures. Arechvo et al. (2013) increased pressure within the auditory canal in ostrich (*Struthio camelus*) from 0 to 2 kPa. The average columella footplate displacements were 190 µm at 0.5 kPa, 270 µm at 1 kPa, and 310 µm at 1.5 kPa. When pressure within the auditory canal was increased and decreased, bending occurred in the extrastapedius while Platner's ligament limits the displacement of the columella footplate. Claes et al. (2017) showed that ME pressure in chickens and mallards is ventilated only once every 1 to 3 minutes, indicating that these birds have to cope with the ME pressure conditions used in the presented study. In the present study on chickens, quasi-static pressure changes were induced in the intracranial air cavities, interaural pathway, and hence both the MEs simultaneously, as all these systems are connected (Wada, 1923; Schwartzkopff, 1955; Counter and Borg, 1979). After increasing ME pressure (conform decrease of pressure in the auditory canal) we observed that the tympanic membrane bulges laterally and the conical tip of the membrane also displaces laterally. A linear translation and a very small rotation of the columella could be observed indicating a largely piston-like motion. At an increase of 1 kPa in ME pressure, 63% of the maximal displacement (at 1.5 kPa) of the extrastapedius and 71% of the maximal movement of the columella footplate was observed. At 1 kPa, extrastapedius displacements were 2.4 times larger than columella displacements, about the magnitude found in Pohlman (1921) and Claes et al. (2017). When ME pressure was increased further only small lateral displacements of the extrastapedius and columella footplate were observed. The displacements are limited in magnitude by both the Platner's ligament becoming tense and by the annular ligament which connects the columella footplate with the oval window. Due to the hyaline cartilage in the extracolumella, bending movement is not only possible between the extracolumella and columella but also at the processi of the extracolumella (Saunders, 1985; Mills, 1994; Starck, 1995; Arechvo et al., 2013). After ME pressure was decreased we observed a medial displacement of the tympanic membrane. A linear translation and a small rotation of the columella were observed which indicate that the columella footplate undergoes a predominantly piston-like motion. At 1 kPa, extrastapedius deformations were 11 times larger than columella footplate displacements. The annular ligament likely protects the inner ear by limiting the displacement of the footplate so the footplate cannot penetrate too deep. At a decrease of 1 kPa in ME pressure, 94% of the maximal displacement (at 1.5 kPa) of the extrastapedius and 100% of the maximal movement of the columella footplate was observed. When ME pressure was decreased further only a small increase in medial displacement was observed. The small rotation angles of the columella footplate support the piston-like motion theory posed by Pohlman (1921) and not the rocking-motion theory posed by Gaudin (1968). In birds, both extrastapedius and columella footplate displacements caused by ME pressure fluctuations show non-linear S-shaped response curves as function of pressure which also indicate the non-linear response characteristics of the ME components. Magnitude of extrastapedius and columella amplitude at negative pressure in the ME are significantly larger than the displacements at overpressure.

The larger displacements of the umbo and smaller displacements of the stapes in humans compared with rabbits can be attributed to the larger tympanic membrane in humans (56 – 85 mm^2 (Gan et al., 2004); rabbit: 32 mm^2 (Marcusohn et al., 2006)) but also to a difference in stiffness of the ossicular chain (Dirckx et al., 2006). The gerbil however, seems to be an exception with a peak-to-peak displacement of 300 µm of the umbo with only a tympanic membrane surface area of 19 mm^2 (Cohen et al., 1992). However, looking at the peak-to-peak displacement of the extrastapedius of the chicken's ME and comparing this to the peak-to-peak displacement of the umbo of the rabbit (similar tympanic membrane surface area), we see that the displacement in chickens is 10 times larger. Scaling the surface area of the tympanic membrane in gerbils to the same size of the chicken's tympanic membrane, peak-to-peak amplitudes of the deformations of the tympanic membrane are still almost 3.7 times smaller in gerbils. This can indicate that the ME system in birds has an ever higher flexibility than the 3 ossicle system in mammals. Scaling the mammalian maximal displacement amplitude of the umbo and stapes to the same magnitude of the maximal displacement amplitude of the extracolumella and columella footplate in chickens show that when ME pressure is increased the ME components seem to be more flexible in chickens as maximal displacement is reached at a lower increased ME pressure than in mammals. Comparing mammalian and avian linear displacements when ME pressure is decreased indicates similar flexibility of the avian ME components.

The results show that the quasi-static displacements of the columella are larger than the stapes displacement in the mammalian ear. This can be expected, as the mammalian ear contains a three-ossicle system which acts as a high-pass filter, reducing quasi-static motions of the footplate when the eardrum is deformed. The flexibility of the extracolumella gives the avian ear another unique feature to buffer static motions at the level of the footplate, which is not present in the mammalian ear. Still, the results show that the inner ear of birds is more prone to quasi-static inputs than the mammalian ear. The inner ear in birds is straight, in contrast to the coiled mammalian cochlea, and the round window in mammals is far smaller than its counterpart in the avian ear. From a hydrodynamic standpoint this might make it easier for the avian inner ear to cope with large displacements at the level of the columella footplate.

The tympanic membrane in mammals is conically shaped with the tip pointing inwards (Decreamer et al., 1991). In birds the tympanic membrane is also conically shaped but the tip is pointing outwards. This anatomical difference can be the main cause of the difference in the S-shape of the pressure-displacement curves between mammals (smaller medial than lateral displacements) and birds (larger medial than lateral displacements). An outward pointing tip of the tympanic membrane can make the tympanic membrane stretch at negative pressure in the auditory canal, but make it easy to bend and balloon at overpressure.

These findings can indicate the importance of including a compliant ‘extracolumella’ or a hinge-like structure within the design of a flexible total ossicular replacement prosthesis in human surgery as an effective method to decrease the potentially damaging of the inner ear by the stapes footplate, as was already was suggested by Beleites et al. (2007) and Arechvo et al. (2013).

Acknowledgements

This research was funded by the Research Foundation of Flanders (FWO), grant number G049414N and 11T9316N. The special research fund of the Ghent University (BOF-UGent) is acknowledged for the financial support of the UGCT Centre of Expertise (BOF.EXP.2017.0007). We want to thank Iván Josipovic for his technical assistance.

References

Arechvo, I., Zahnert, T., Bornitz, M., Neudert, M., Lasurashvili, N., Simkunaite-Rizgeliene, R., 2013. The ostrich middle ear for developing an ideal ossicular replacement prosthesis. Eur. Arch. Otorhinolaryngol. 270, 37-44. doi: 10.1007/s00405-011-1907-1.

Ades, H.W., Axelsson, A., Baird, I., Békésy, G.V., Boord, R.L., Campbell, C.B.G., Densert, O., Eldredge, D.H., Engström, H., Fex, J., Harrison, J.M., Henson, O.W., Howe, M.E., Iurato, S., Michelsen, A., Møller, A.R., Pfeiffer, R.R., Rauch, S., Rauch, I., Shaw, E.A.G., Wersäll, J., Wever, E.G., 2012. Auditory System: Anatomy Physiology (Ear). Berlin, Germany: Springer Science & Business Media.

Beleites, T., Bornitz, M., Offergeld, C., Neudert, M., Hüttenbrink, K.B., Zahnert, T., 2007. Experimental investigations on middle ear prostheses with an integrated micro joint. Laryngol. Rhinol. Otol. 86, 649-654. doi: 10.1055/s-2007-966514.

Claes, R., Muyshondt, G.G.P., Dirckx, J.J.J., Aerts, P., 2017. Deformation of birds middle ear structures under static pressure loads, and potential regulation mechanisms. Zoology, in press. doi: 10.1016/j.zool.2017.11.003.

Cohen, Y.E., Bacon, C.K., Saunders, J.C., 1992. Middle ear development III: Morphometric changes in the conducting apparatus of the Mongolian gerbil. Hear. Res. 62, 187-193. doi: 10.1016/0378-5955(92)90185-P.

Counter, S.A., Borg, E., 1979. Physiological activation of the stapedius muscle in Gallus gallus. Acta. Otolaryngol. 88, 13-19. doi: 10.3109/00016487909137134.Decreamer, W.F., Dirckx. J.J.J., Funnell, W.R.J., 1991. Shape and derived geometrical parameters of the adult, human tympanic membrane measured with a phase-shift moiré interferometer. Hear. Res. 51, 107-122.

Dierick, M., Van Loo, D., Masschaele, B., Van den Bulcke, J., Van Acker, J., Cnudde, V., Van Hoorebeke, L., 2014. Recent micro-CT scanner developments at the UGCT. Nucl. Instrum. Methods Phys. Res. B. 324, 35-40. doi: 10.1016/0378-5955(91)90010-7.

Dirckx, J.J.J., Decreamer, W.F., 1991. Human tympanic membrane deformation under static pressure. Hear. Res. 51, 93-105. doi: 10.1016/0378-5955(91)90009-X.

Dirckx, J.J.J., Decreamer, W.F., 2001. Effect of middle ear components on eardrum quasi-static deformation. Hear. Res. 157, 124-137. doi: 10.1016/S0378-5955(01)00290-8.

Dirckx, J.J.J., Buytaert, J.A.N., Decreamer, W.F., 2006. Quasi-static Transfer Function of the Rabbit Middle Ear, Measured with a Heterodyne Interferometer with High-Resolution Position Decoder. Jaro. 7, 339-351. doi: 10.1007/s10162-006-0048-5.

Gan, R.Z., Feng, B., Sun, Q., 2004. Three-Dimensional Finite Element Modeling of Human Ear for Sound Transmission. Ann. Biomed. Eng. 32, 847-859. doi: 10.1023/b:abme.0000030260.22737.53.

Gaudin, E.P., 1968. On the middle ear of birds. Acta Otolaryngol. 65, 316-326. doi: 10.3109/00016486809120971.

Hüttenbrink, K.B., 1988. The Mechanics of the Middle-Ear at Static Air Pressure: The Role of the Ossicular Joints, the Function of the Middle-ear Muscles and Behavior of Stapedial Prostheses. Acta. Otolaryngol. 105, 1-35. doi: 10.3109/00016488809099007.

Rosowski, J.J., Lee, C.Y., 2001. The effect of immobilizing the gerbil's pars flaccida on the middle ear's response to static pressure. Hear. Res. 174, 183-195. doi: 10.1016/S0378-5955(02)00655-X.

Manley, G.A., 1990. Peripheral Hearing Mechanisms in Reptiles and Birds. Zoophysiology, Springer-Verlag, Heidelberg, New York. doi: 10.1007/978-3-642-83615-2.

Marcusohn, Y., Dirckx, J.J.J., Ar, A., 2006. High-Resolution Measurements of Middle Ear Gas Volume Changes in the Rabbit Enables Estimation of its Mucosal CO2 Conductance. J. Assoc. Res. Otolaryngol. 7, 236-245. doi: 10.1007/s10162-006-0038-7.

Mills, R., 1994. Applied comparative anatomy of the avian middle ear. J. R. Soc. Med. 87, 155-156. doi: 10.1177/014107689408700314.

Møller, A.R., 1974. Function of the Middle ear, Auditory System. Berlin, Germany: Springer.

Murakami, S., Gyo, K., Goode, R.L., 1997. Effect of Middle Ear Pressure Change on Middle Ear Mechanics. Acta Otolaryngol. 117, 390-395. doi: 10.3109/00016489709113411.

Muyshondt, P.G.G., Claes, R., Aerts, P., Dirckx, J.J.J. 2017. Quasi-static and dynamic motions of the columellar footplate in ostrich (Struthio camelus) measured ex vivo. Hear. Res., in press. doi: 10.1016/j.heares.2017.11.005.

Norberg, R., 1978. Skull asymmetry, ear structure and function, and auditory localization in Tengmalm's owl, Aegolius funereus (Linne). Phil. Trans. R. Soc. Lond. 282, 325-410. doi: 10.1098/rstb.1978.0014.

Pohlman, A.G., 1921. The position and functional interpretation of the elastic ligaments in the middle-ear of Gallus. J. Morphol. 35, 229-262.

Rosowski, J.J., 1996. Models of External- and Middle-ear Function, Auditory Computation. New York, United States: Springer.

Saunders, J.C., 1985. Auditory structure and function in the bird middle ear: an evaluation by SEM and capacitive probe. Hear. Res. 18, 253-268. doi: 10.1016/0378-5955(85)90042-5.

Saunders, J.C., Duncan, R.K., Doan, D.E., Werner, Y.L., 2000. The middle ear of reptiles and birds. In: Dooling, R.J., Fay, R.R., Popper, A.N. (Eds.), Comparative Hearing: Birds and Reptiles. Springer, New York, United states, pp. 13-69. doi: 10.1007/978-1-4612-1182-2_2.

Schwartzkopff, J., 1955. On the Hearing of Birds. The Auk. 72, 340-347. doi: 10.2307/4081446.

Smith, G., 1904. The middle ear and columella in birds. QJ. Microsc. Sci. 48, 11-22.

Starck, J.M., 1995. Comparative anatomy of the external middle ear of palaeognathous birds. Adv. Anat. Embryol. Cell. Biol. 131, 1-137.

Teoh, S.W., Flandermeyer, D.T., Rosowski, J.J., 1997. Effects of pars flaccida on sound conduction in ears of Mongolian gerbil: Acoustic and anatomical measurements. Hear. Res. 106, 39-65. doi: 10.1016/S0378-5955(97)00002-6.

Wada, Y., 1923. Beiträge zur verleichenden Physiologie des Gehörorgane. Pflügers Archiv. 202, 46-69.